RGNZ/MGPB

Extensional Tectonic Investigation based on Gravity and Magnetic Data Analysis in the Gulf of Tomini, Indonesia

Rudarsko-geološko-naftni zbornik
(The Mining-Geology-Petroleum Engineering Bulletin)
UDC: 550:03
DOI: 10.17794/rgn.2023.4.1

Original scientific paper

Accep Handyarso[1,2]; Haryadi Permana[1,3]; Mustafa Hanafi[1,4]; Purnama Sendjaja[1,2]; Muhammad Maruf Mukti[1,3]

[1] Research Center for Geological Resources, National Research and Innovation Agency (BRIN) of the Republic of Indonesia. Samaun Samadikun Science and Technology Center, BASICS Tower 2. Jalan Sangkuriang Bandung Indonesia. 40135.

[2] Ex-Center for Geological Survey, Geological Agency, Ministry of Energy and Mineral Resources (MEMR) of the Republic of Indonesia. Jalan Diponegoro, Bandung, Indonesia. 40122.

[3] Ex-Research Center for Geotechology, Indonesian Institute of Science of the Republic of Indonesia. Jalan Sangkuriang, Bandung, Indonesia. 40135.

[4] Ex-Marine Geological Institute, Research and Development Agency, Ministry of Energy and Mineral Resources (MEMR) of the Republic of Indonesia. Jalan Dr. Djundjunan 236, Bandung, Indonesia. 40174.

ORCID: AH (https://orcid.org/0000-0001-9449-490X), HP (https://orcid.org/0000-0002-4604-3298), MH (https://orcid.org/0000-0002-2442-6095), PS (https://orcid.org/0000-0001-6867-427X), MMM (https://orcid.org/0000-0002-9467-537X).

Abstract

The enigmatic genesis of Sulawesi Island remains a debate among earth scientists up to the present day. The Northern Arm of Sulawesi is designated as a volcanic province, while the Eastern Arm is identified as an ophiolite zone along with several micro continental fragments. However, the tectonic relationship in the marine area between these two arms is not clearly defined. The existence of isolated volcanic islands, namely the Una-Una and Togian islands increases the complexity of the area. A regional study utilizing gravity and magnetic methods is needed in the Gulf of Tomini, North Sulawesi, Indonesia. Therefore, a comprehensive analysis was conducted, involving 3D inverse modelling and Moho depth estimation based on the Parker-Oldenburg algorithm using 3D Euler deconvolution to obtain the average depth of causative bodies. As a result, the presence of extensional tectonics were revealed and identified as multiple parallel dextral strike-slip faults across the study area. All of these faults show northwest-southeast lineaments consistent with the existing seismic sections. The extensional tectonic mechanism triggers crustal thinning and rifting, leading to the build-up of graben structures such as the Gorontalo, Tomini, and Poso basins. Additionally, it influences volcanic activity around the Togian and Una-Una islands. The major axes of the inferred opening area are oriented in the northeast-southwest direction, perpendicular to the lineaments of these faults. The opening area coincides with the orientation of Lalanga and Togian ridges. Finally, a regional geological structure is proposed across the Gulf of Tomini linking both the Northern and Eastern arms of Sulawesi.

Keywords:
Gravity; Magnetic; Mohorovičić discontinuity; Extensional tectonic; Gorontalo-Tomini Basin

1. Introduction

The Gulf of Tomini as a study area, located between the Northern Arm and the Eastern Arm of Sulawesi Island, Indonesia, is defined as a geologically complex region with abundant tectonic activities for both subduction-collision zones and an active extensional regime (**Cottam et al., 2011; Pholbud et al., 2012; White et al., 2014; Sendjaja et al., 2020**). These tectonic activities resulted in an island with a unique shape resembling the letter K (**White et al., 2014**). The island consists of several arms, namely the Northern Arm of Sulawesi defined as a volcanic province, Western Sulawesi consisting of a volcanic province and continental basement, Central Sulawesi recognized as a metamorphic-belt region, the Eastern Arm of Sulawesi defined as ophiolite, and other micro continental fragments (Eastern Arm and Buton), as shown in **Figure 1**. Several deep marine bays are located between the arms, such as Gorontalo Bay, Tomini Gulf, Tomori Bay, and Bone Bay (**Pholbud et al., 2012; Watkinson et al., 2012; Nugraha and Hall, 2018**). All of these arms and bays are sliced by several major strike-slip faults, such as the Palu-Koro Fault, the Lawanopo Fault, the Walanae Fault, the Kolaka Fault, the Gorontalo Fault, the Matano Fault, and the Balantak Fault (**White et al., 2014**).

The geological structures surrounding Tomini Bay are relatively well defined and have been the subject of

Corresponding author: Accep Handyarso
e-mail address: accep.handyarso@brin.go.id

extensive research studies (**Hamilton, 1979; Walpersdorf et al., 1998a; Djajadihardja et al., 2004; Rudyawan et al., 2014; White et al., 2014; Nugraha and Hall, 2018; Song et al., 2022**). However, the sea-to-land ratio of the Sulawesi region is dominated by deep marine waters including the Gulf of Tomini area, which still lacks information. Consequently, various theories regarding the genesis of Togian and Una-Una Islands (Colo Volcano) have been proposed. The existing interpretations are divided into subduction-related volcanoes and non-subduction related volcanoes. In the cases of the subduction-related volcanoes scenario, there are several possibilities that can trigger volcanic activity. These possibilities include the south-eastward dipping of the dormant subduction slab of the Celebes Sea Plate (CSP), the East Sangihe subduction slab associated with the westward motion of the Molucca Sea Plate (MSP), and the subduction slab of the remaining Banggai-Sula Microcontinent (BSM), which moves northwestward beneath the Eastern Arm of Sulawesi (**Sendjaja et al., 2020**). According to the volcanic products found in Una-Una Island, it is inferred that the Colo Volcano shares similar characteristic with the volcanic province of the Northern Arm of Sulawesi. Therefore, it was concluded that the origin of Colo Volcano is derived from the subduction of the Celebes Sea Plate (CSP) with south-eastward movement (**Sendjaja et al., 2020**). The scenario of non-subduction-related volcanoes correlates with the extensional tectonic mechanism. The presence of medium K to shoshonite magmatic affinity has been identified based on geochemical analysis in the same area, supporting the scenario of non-subduction-related volcanoes (**Cottam et al., 2011; Watkinson et al., 2012**). Several studies have reported that the volcanism in the Togian and Una-Una islands is the result of the extensional tectonic mechanism during the Pliocene and Pleistocene periods (**Cottam et al., 2011; Pholbud et al., 2012**). It has been inferred that the volcanism is not associated with the CSP subduction slab due to its geometric configuration, which is situated at a depth beyond the range where partial melting occurs. However, these conclusions do not provide any explanation about the mechanism of extensional tectonics in the Gulf of Tomini. On the other hand, despite being in the same area, the geochemical analyses yield conflicting results regarding the origin of the Colo Volcano in Una-Una Island.

The tectonic relationship between the Northern Arm and Eastern Arm of Sulawesi has never been clearly defined in previous research. The study area presented in this paper encompasses the Gulf of Tomini, which is situated between these two arms. The existence of the Gorontalo, Tomini, and Poso basins cause the deep marine bay areas believed to reserve geological resource potential. This potential requires massive geological research and exploration efforts. Therefore, the objective of this study is to provide a comprehensive snapshot of the current tectonic settings across the Gulf of Tomini based on gravity-magnetic datasets and to establish correlations with the existing interpretations of geological structure on-land. As a result, a comprehensive synthesis of the geological structure interpretation over the study area and its surrounding will be provided. The study results will contribute to a deeper understanding of the tectonic settings of the region. Furthermore, it will serve as a valuable guide for both exploration of geological resources and the mitigation of geological disasters in the study area.

2. Geological Settings

Tectonically, Northern Sulawesi is formed due to the convergence of a triple junction involving several plates, including the Eurasian Continental Plate (ECP), the Celebes Sea Plate (CSP), the Australian Banda Arc Plate (ABP), and the Philippine Sea Plates (PSP). The interactions and collisions between these plates have played a significant role in the geological evolution of Sulawesi Island. The tectonic system of Sulawesi Island is characterized by the westward motion of the PSP, the south-eastward movement of the ECP with the western region acting as a relatively steady reference point, the southward movement of the CSP, and the north-westward movement of the ABP. These plate interactions form a fascinating and enigmatic tectonic framework within Sulawesi Island (**Walpersdorf et al., 1998a; 1998b; Kopp et al., 1999; Kusnida, 2008; Martosuwito, 2012**). The existence of isolated volcanic island in the study area, i.e. Una-Una and Togian islands increase the complexity of the tectonic system within the arc (**Katili et al., 1963; Cottam et al., 2011; Sendjaja et al., 2020**). Extensive research on the tectonic evolution of Sulawesi Island suggests that the region has passed through a complex tectonic deformation due to the interaction among plates.

Several research results show a relationship between the rapidly subsiding Gorontalo Basin, regional extensional tectonics, and rotation of the Northern Arm away from the Eastern Arm of Sulawesi in a clockwise direction (**Cottam et al., 2011; Pholbud et al., 2012; Advokaat et al., 2017**). All of these occurrences are happening at the present day and have been substantiated by time-lapse GPS measurements. Most earth scientists believe that the continuous northward slab rollback at the hinge of the North Sulawesi Trench resulted from the reversal of southward subduction of the Celebes Sea Plate (CSP), which has been occurring since the Pliocene (**Advokaat et al., 2017**). These conditions cause faults in both the Northern and Eastern Arms of Sulawesi, which predominantly have northwest-southeast lineaments, such as the Gorontalo Fault, the Teba Fault, the Harapan Fault, the Rompi Fault, the Sabo Fault, the Balantak Fault, etc. (**Sidarto and Bachri, 2015**), as shown in **Figure 1**. It is inferred that Una-Una Island (Colo Vol-

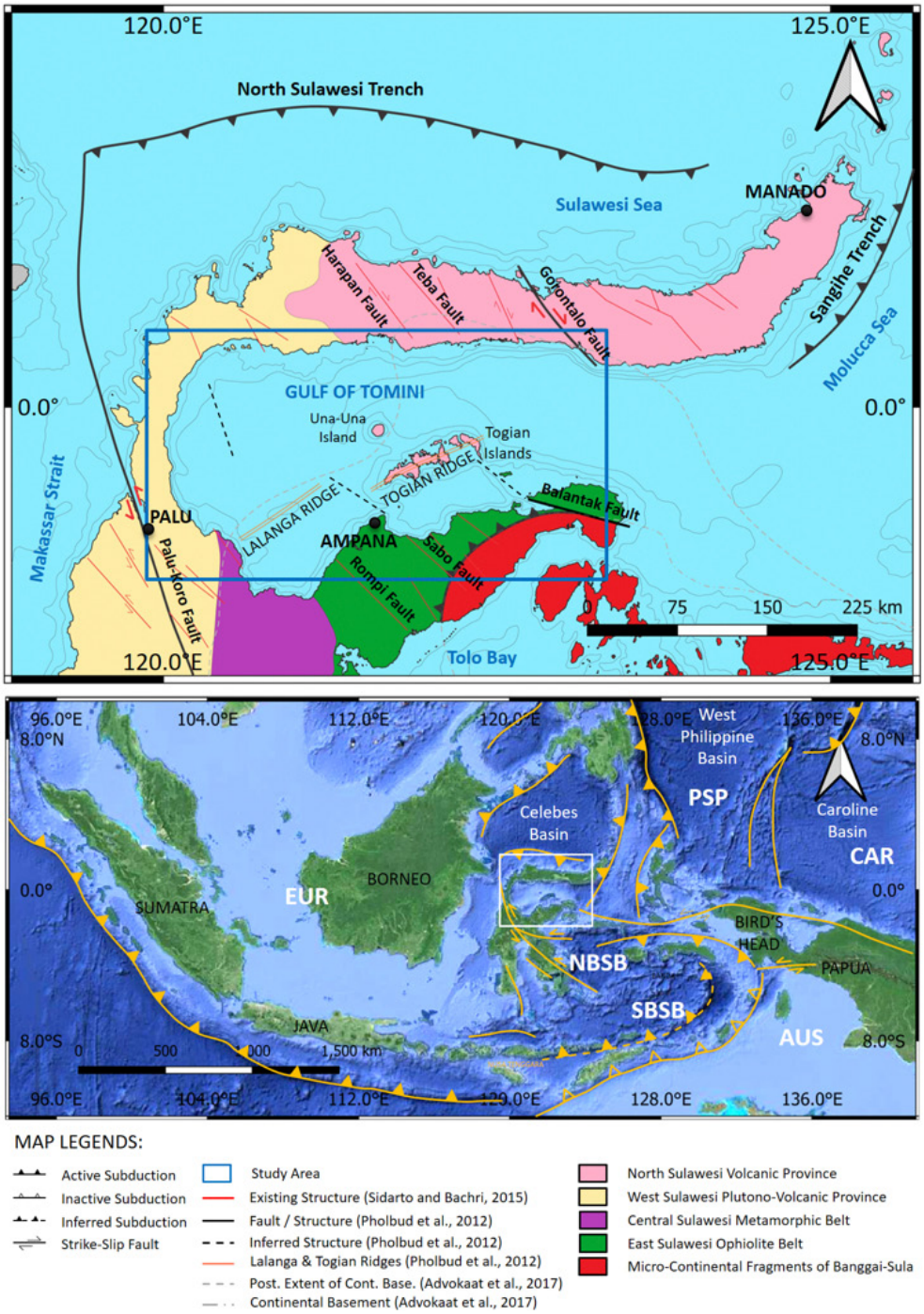

Figure 1: Main tectonic features of the Gulf of Tomini are marked with the black and orange lines (from **Pholbud et al., 2012**), overlaid with the existing onshore geological structures of the Northern Arm and the Eastern Arm of Sulawesi-MEMR, which are marked with the red lines (from **Sidarto and Bachri, 2015**). Northern Sulawesi's subdivisions are color-coded on the map with explanations in the legend. Inset map shows the regional geological structures with several major plates and trenches (from **Hinschberger et al., 2005**). Several major plates are marked with CAR (Caroline Sea Plate), PSP (Philippine Sea Plate), EUR (Eurasian Continental Plate), AUS (Australian Continental Plate), and NBSB-SBSB (North/South Banda Sea Basin). The study area is outlined by a blue rectangle and covered the marine area known as the Gulf of Tomini. The Lalanga and Togian ridges inferred from bathymetric data are shown as orange double lines.

cano) might be an expression of crustal thinning, while the Lalanga Ridge has been successfully identified based on bathymetric datasets and defined as a carbonate reef with several pinnacle reefs and limestones (**Pholbud et al., 2012**).

According to the plate tectonic reconstructions, during the early Cretaceous (120 Ma), Southwest Borneo (SWB) and East Java and West Sulawesi (EJWS) moved away from Australia and approached the margin of Sundaland or Eurasia (**Hall, 2012; Baillie and Decker,**

2022). The EJWS converged with SWB and joined with Sundaland in the late Cretaceous (85 Ma). A subduction with the northwest dipping direction occurred and was marked by volcanic activity in West Sulawesi and Sumba at around 65 Ma. Around 45 Ma, the Celebes Sea Plate (CSP) and Philippine Sea Plate (PSP) were spreading in a back-arc setting, while the Ceno-Tethys subducted northwards from Sumatra to Halmahera. In the late Oligocene period (around 25 Ma), the Sula spur was on the verge of making contact with the Northern Arm of the Sulawesi volcanic arc as the beginning of a collision between Australia and Southeast Sundaland. In the middle Miocene (around 15 Ma), the seafloor spreading of the Sulu Sea occurred in a back-arc setting due to the rollback of Celebes Sea Plate (CSP) subduction. In the late Miocene (around 10 Ma), the rollback mechanism also occurred in the Banda embayment and formed the North Banda Sea due to the extension of the Sula spur. During the same period, Andaman seafloor spreading was also occuring. During the Pliocene period (around 5 Ma), the South Banda Sea formed as a result of the rollback into the Banda embayment, leading to extension in the region. The subduction of the Molucca Sea Plate was almost complete during this time, and the Halmahera and Sangihe arcs were prepared for collision. Finally, the regional tectonic settings that formed Sulawesi Island are comparable to the current tectonic conditions, as shown in **Figure 1**. Sulawesi Island underwent significant shaping and deformation due to the intensive movement (subduction, collision, and obduction) of the Sula platform (Banggai-Sula Microcontinent). These processes resulted in a clockwise rotation of the Northern Arm of Sulawesi and the development of the North Sulawesi trench since the early Miocene up to the present time (**Silver et al., 1983**). In the early Pliocene, a collision occurred between Sulawesi and Australia (New Guinea Micro Plate), leading to the significant transformation of Sulawesi into an island. As a result of this collision, Sulawesi experienced severe deformation, causing its convex side to face towards the continent. Additionally, obduction of ophiolite occurred in the Eastern Arm of Sulawesi Island (**Katili, 1978**).

In accordance with the geological consensus regarding the tectonic settings of Sulawesi Island in the past decade, it has been established that the island is primarily a result of contractional, strike-slip tectonics, accompanied by subsequent rotation (**Baillie and Decker, 2022**). The tectonic evolution regime of Sulawesi Island can be divided into two main periods. Firstly, during the Mesozoic-Paleogene period, there was significant tectonic activity that played a role in the main blocks or platform forming the island. Secondly, during the Neogene period, which started from the middle Miocene to present time, there was movement and interaction among these blocks or platforms, which contributed to the forming of Sulawesi Island (**Hinschberger et al., 2005; Baillie and Decker, 2022**). Massive time-lapse GPS measurements have been conducted for more than a decade with various purposes (**Puntodewo et al., 1994; Walpersdorf et al., 1998a; 1998b; Rangin et al., 1999; Socquet et al., 2006**). In addition to monitor the local movement of the Palu-Koro Fault, GPS measurements have also confirmed the validity of the "Salami Slicer" model. This model suggests that the collision in Sulawesi Island is primarily driven by terranes from the east as the product of continent dispersion, which are drifted by the seafloor spreading mechanism (**Pigram and Panggabean, 1984; Baillie and Decker, 2022**). Furthermore, the GPS data measurements have also identified a small number of crustal blocks that show rapid rotation, which are confined within the Palu-Koro and Lawanopo fault systems (**Socquet et al., 2006; Baillie and Decker, 2022**). The rotation mechanism is caused by the coupled system of strike-slip and thrust faults (**Silver et al., 1983; Hamilton, 1979; Baillie and Decker, 2022**). Travel Time Tomography plays an important role in determining the characteristics of the subduction slab beneath the Earth's surface. The west-east double subductions beneath the Molucca Sea Plate have been successfully imaged using this method (**Rachman et al., 2022**).

3. Methodology

The gravity dataset utilized in the study is obtained from the global satellite gravity mission TOPEX/POSEIDON. The data are collected in the form of Free Air Anomaly (FAA) and topography datasets, with a lateral resolution of approximately 1.5 km (**Oceanography, 2023**). Both the FAA and topography/bathymetry datasets are processed and combined to calculate the Complete Bouguer Anomaly (CBA) using the FA2BOUG software, which is implemented in a FORTRAN code (**Fullea et al., 2008**). To cover both sea and land gravity datasets, a density value of 1021.6 kg/m^3 is selected for the gravity data reduction. This density value is chosen based on the Parasnis method (**Rao and Satyanarayana Murty, 1973**). The Radially Averaged Power Spectrum (RAPS) plays a crucial role in the separation of regional-residual gravity data. The calculation of the method can be performed using different techniques, such as the wavenumber filtering technique or the moving average technique with a specified window size. The Total Magnetic Intensity (TMI) data are converted to Reduction to Pole (RTP) using inclination and declination values based on the International Geomagnetic Reference Field (IGRF) provided by the National Oceanic and Atmospheric Administration (NOAA). In this study, the RTP transformation from the TMI data is performed using specific inclination and declination values. The inclination value used is -16.8352°, while the declination value used is 0.9001°. The magnetic data acquisition was conducted around 2010/2011 by the Marine Geological Institute (MGI), Geological Agency, Indonesia (Ministry of Energy and Mineral Resources-MEMR). The data

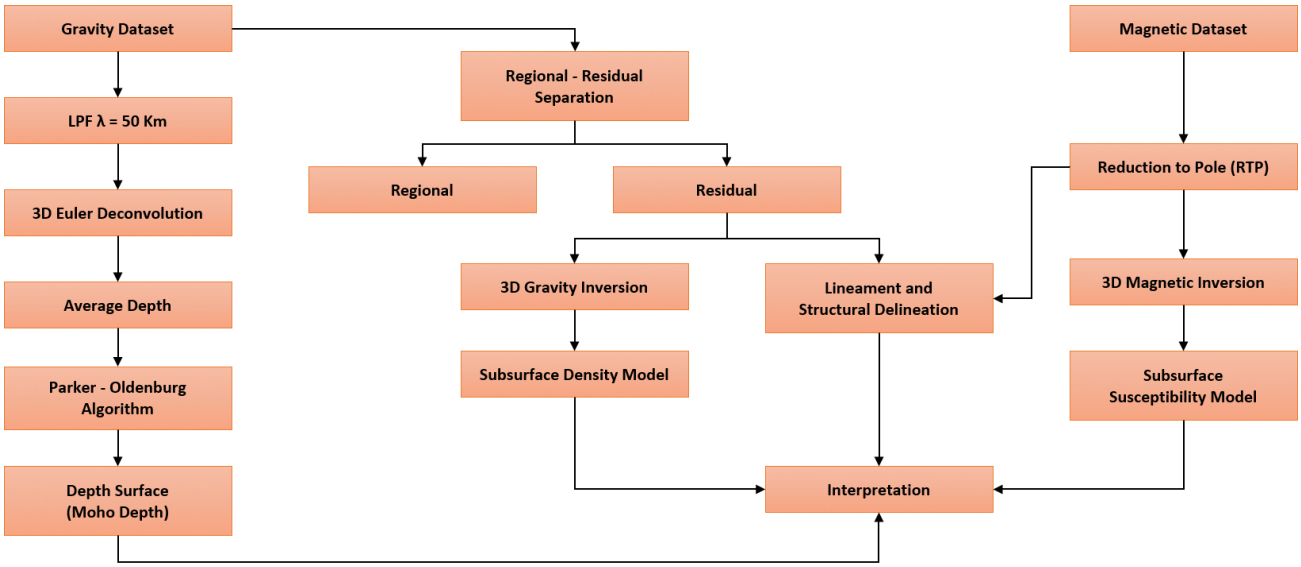

Figure 2: Workflow implemented within this research

was subsequently compiled and incorporated into the Magnetic Anomaly Map of East and Southeast Asia Revised Version (3rd Edition) in the year of 2021 by Coordinating Committee for Geoscience Programmes (CCOP) in East and Southeast Asia and Geological Survey of Japan (GSJ), National Institute of Advanced Industrial Science and Technology (**CCOP and GSJ, 2021**).

In general, the research methodology (framework) involves optimizing the utilization of gravity and magnetic datasets through three main parts (see **Figure 2**). These parts include Mohorovičić discontinuity (Moho-depth) estimation based on the gravity dataset, conducting a single 3D inversion for both the gravity and magnetic data to visualize the distribution of density contrast and susceptibility below the surface, and performing lineament analysis of anomalies in the study area using gravity and magnetic datasets. The Moho depth estimation is calculated based on gravity anomalies, which are obtained by applying a low pass filter to the Complete Bouguer Anomaly (CBA) datasets. This filtering process is useful to obtain a long-wavelength gravity anomaly. The calculation of the Moho depth requires an initial depth interface, which is refined iteratively through the calculation using the Parker-Oldenburg algorithm (**Gómez-Ortiz and Agarwal, 2005; Chen et al., 2021**) or based on 3D gravity inversion using GROWTH 2.0 (**Ashena et al., 2018**). The initial depth interface use the average depth value of the causative body, which is derived from the spectral analysis or the 3D Euler deconvolution (**Reid et al., 1990; Beiki, 2010; Golshadi et al., 2016; Parang et al., 2016**) instead of using shear wave tomography (**Ardestani and Mousavi, 2023**). The spatial analysis of the Moho depth distribution is integrated with the findings from lineament analysis and 3D inversion to provide a comprehensive explanation of the tectonic settings within the study area. The lineament analysis is performed by comparing the residual gravity anomaly with the RTP magnetic anomaly. In this case, the residual gravity anomaly is obtained from the regional-residual data separation, while the RTP magnetic anomaly is a conversion result from the TMI using specified inclination and declination values. The identification of lineament anomaly patterns was conducted based on forward modelling using both gravity and magnetic datasets (**Handyarso and Saleh, 2017; Handyarso, 2022, 2023**). The 3D gravity inversion is performed using low pass filtered CBA dataset instead of the result from regional-residual data separation, while the 3D magnetic inversion utilizes the RTP anomaly in the study area. These results are subsequently cross-validated and integrated to provide a comprehensive description of the subsurface conditions. Seismic data are used to confirm the results, ensuring the accuracy and reliability of the interpretation results. Lastly, the structural interpretation is superimposed onto the Digital Elevation Model (DEM) in a 3D perspective to visually verify the findings as an additional approach to confirm the results.

3.1. Moho depth estimation

3.1.1. Frequency Filtering

Frequency filtering based on the Fourier Transform plays an important role in the processing of potential field data. The aims of these filtering stages are to remove unwanted noise and to enhance the desired signals. In this study, the filtering technique was performed based on the wavelength (λ) filtering approach. The long wavelength cut-off used for this purpose is within the range of 50-100 km, serving as a Low-Pass Filter (LPF) to represent the Mohorovičić discontinuity interface. The long wavelength trend contained in the data will correspond to any known large structures close to the surface, which are typically associated with the Mohorovičić discontinuity (**Lefort and Agarwal, 2000**). The

Fourier Transform, which converts data from the spatial domain into frequency domain can be mathematically expressed using **Equation 1**.

$$F(k) = \sum_{n=0}^{N-1} f(x_n) e^{-i\frac{2\pi k}{N}n} \quad (1)$$

where:

$f(x_n)$ – Potential field dataset in spatial domain,
N – Period,
$k = 1/\lambda$ – Wavenumber,
λ – Wavelength,
$\frac{k}{N}$ – Frequency,
$F(k)$ – Potential field dataset in frequency domain.

The spectral analysis formulation of the potential field for both frequency-based and wavelength-based filtering can be calculated using **Equation 2**. This equation known as the Radially Averaged Power Spectral (RAPS), is expressed in the form of the Fourier Transform of the potential field under the assumption of a horizontal plane (**Blakely, 1995; Parlak and Elmas, 2023**).

$$F[g_z] = 2\pi G \Delta\rho e^{|k|(z_0 - z)},\ z > z_0 \quad (2)$$

where:

$F[g_z]$ – Fourier Transform of gridded gravity anomaly,
G – Universal gravity constant,
$\Delta\rho$ – Density contrast between two layers,
z_0 – Height of the observation points,
z – Depth of the causative body.

Equation 2 can be simplified to **Equation 3**. Additionally, **Equation 4** expresses **Equation 3** in terms of the natural logarithm on both sides, resulting in a linear relationship between the wavenumber and spectrum amplitude.

$$A = Ce^{|k|(z_0 - z)},\ z > z_0 \quad (3)$$

$$\ln \ln A = |k|(z_0 - z) + \ln \ln C,\ z > z_0 \quad (4)$$

where:

A – Spectrum amplitude,
C – Constant,
$k = 2\pi/\lambda$ – Wavenumber,
$\lambda = n\Delta x$ – Wavelength,
n – Window size,
Δx – Interval.

The slope of the linear relationship between the wavenumber and spectrum amplitude in the Radially Averaged Power Spectral (RAPS) analysis provides an estimation of the average depth of the causative body. Hence, the average depth of the anomaly source can be estimated using RAPS approximation.

3.1.2. 3D Euler Deconvolution

The 3D Euler deconvolution method is widely used in potential field data analysis, particularly in gravity and magnetic data interpretations. It provides an estimation of the location and depth of the causative bodies (**Reid et al., 1990; Blakely, 1995; Reid, 1998; Golshadi et al., 2016**). The 3D Euler deconvolution concisely can be expressed using **Equation 5**.

$$(x_0 - x)\partial g/\partial x + (y_0 - y)\partial g/\partial y + (z_0 - z)\partial g/\partial z = N(B - g) \quad (5)$$

where:

x, y and z – Coordinates of the source location,
x_0, y_0 and z_0 – Coordinates of the observation points,
B – Base level or Background value,
N – Structural Index (SI) or degree of the homogeneity,
g – Gridded potential field measured at observation points, which refers to a gravity or magnetic anomaly.

The structural index measures the decay rate of the potential field from the source as the distance changes (**Golshadi et al., 2016**). This feature can be utilized to distinguish sources from different geometries or shapes. Every shape has a distinct level of "sharpness" relative to its depth, resulting in a unique attenuation rate (**Thompson, 1982; Golshadi et al., 2016**). The type of contact anomaly is assumed to have a structural index (SI) value between 0.0 up to 0.5 (**Thompson, 1982; Yudistira and Grandis, 1998; Golshadi et al., 2016**). The correct assignment of structural index (SI) parameter is significant to the successful implementation of the 3D Euler deconvolution method. As a result, the 3D Euler deconvolution solution provides both lateral locations and depth information.

3.1.3. Parker-Oldenburg Algorithm

The Parker-Oldenburg algorithm is widely used to estimate the depth interface of causative bodies based on gravity datasets (**Gómez-Ortiz and Agarwal, 2005; Kunnummal et al., 2018**). The mathematical representation of the algorithm is expressed using **Equation 6**.

$$F[h(x,y)] = -\frac{F[\Delta g(x,y)]e^{|k|z}}{2\pi G\rho} - \sum_{n=2}^{\infty} \frac{|k|^{n-1}}{n!} F[h(x,y)^n] \quad (6)$$

where:

F [] – Fourier transform 2D discrete,
G – Universal gravitational constant,
ρ – Density contrast across the interface,
$\Delta g(x, y)$ – Gridded gravity anomaly,
$h(x, y)$ – Depth to interface (positive downwards),
z – Average (mean) depth of horizontal interface,
$|k|$ – Absolute value of the wave number.

The equation above allows us to estimate the depth of the Mohorovičić discontinuity interface beneath the surface by means of an iterative calculation process. In the process, it is assumed that the average (mean) depth z as the initial horizontal interface is derived from the 3D Euler deconvolution result. As a comparison, the average

Table 1: Physical parameters of the Causative Bodies used in the Synthetic Modelling (Referenced to **Figure 3**)

	Prism #1 Dimensions		**Prism #2 Dimensions**	
	Start	**End**	**Start**	**End**
Easting X (m)	241572.080	254679.200	250646.240	263753.360
Northing Y (m)	9179240.470	9197381.410	9197381.410	9215522.350
Depth Z (m)	-2519.565	-19640.92	-2519.565	-19640.92
Density Contrast (kg/m^3)	700		700	
Susceptibility (SI)	5.0 e-3		5.0 e-3	

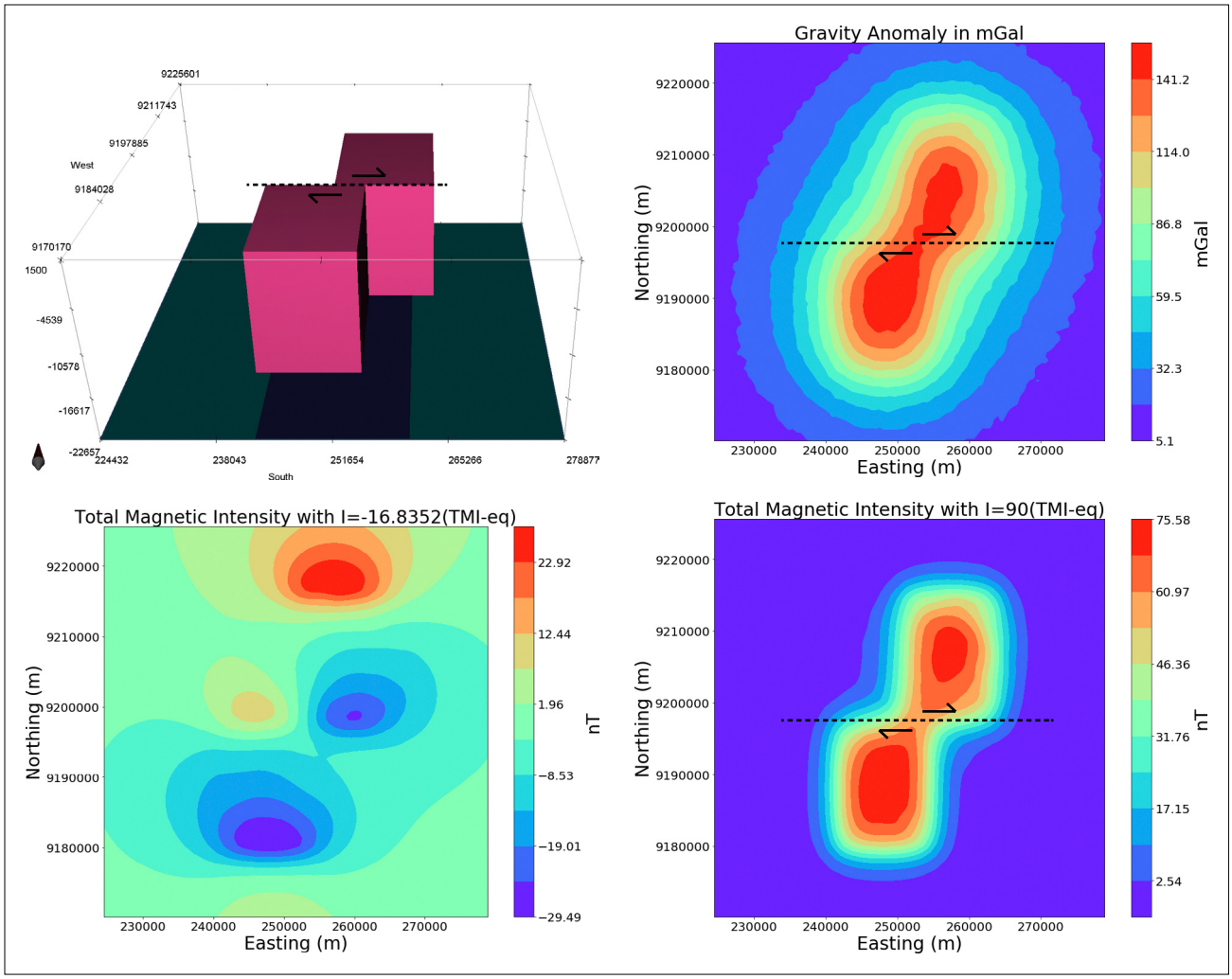

Figure 3: Subsurface model of a dextral strike-slip fault and corresponding model responses calculated based on the rectangular prisms equation proposed by Plouff for gravity forward modelling and Bhattacharyya for magnetic forward modelling (**Blakely, 1995**). The top left image shows the synthetic model designed to simulate the existence of a dextral strike-slip fault. The top right image shows the gravity data response to the synthetic model. The bottom figures show the magnetic data responses of the synthetic model in terms of Total Magnetic Intensity or TMI (bottom left) and Reduction to Pole or RTP (bottom right).

depth in this study is also calculated based on the Radially Averaged Power Spectral (RAPS) of the gravity anomaly, which invoked the Fourier Transform (**Blakely, 1995; Parlak and Elmas, 2023**).

3.2. Gravity and Magnetic Inversion

A forward problem is a synthetic data calculation that arises from the distribution of a particular set of known physical properties, while the inversion is an attempt to recover the distribution of the physical properties based on the given datasets (**Oldenburg and Li, 2005**). Generally, a forward modelling operator produces the model response of the known model parameter distribution with some noises contained in the data expressed in **Equation 7**.

$$d^{obs} = F[m] + e \tag{7}$$

where:

d^{obs} – Response model or field datasets,

F [] – Forward modelling operator, which accommodates the survey design and relevant physical formulation,

m – Model parameter (physical property distribution),

e – Noise associated with the data points.

In the case of gravity and magnetic methods, the forward modelling operators are based on the rectangular prism equation proposed by Plouff for the gravity method and Bhattacharyya for the magnetic method (**Blakely, 1995**). The model parameters or physical properties in our study are correlated with the density contrast (ρ) and susceptibility (χ) distribution beneath the surface. Inverse modelling is also known as the fitting of the model function $F[m]$ from a vector of m as the physical property to a set n number of data points (**Grandis, 2009; Ardestani and Mousavi, 2023**). The solution is approximated by using weighted least square errors between the data points with the predicted dataset. The Gauss-Newton scheme is invoked for minimizing the objective function expressed in **Equation 8**, as described in previous studies (**Grandis, 2009; Ghalehnoee et al., 2017**).

$$m = \underline{W}_m^{-1} \underline{A}^T \left[\underline{A}^T \underline{W}_m^{-1} \underline{A} + \mu \underline{W}_e^{-1} \right]^{-1} \left(d - F[m] \right) \quad (8)$$

where:

$\underline{A}$ – Kernel matrix,

$\underline{W}_m$ – Model weighting matrix, which consists of depth weighting and compactness weighting,

$\underline{W}_e$ – Noise weighting matrix,

μ – Damping factor,

d – Data points vector.

3.3. Lineament analysis

The forward modelling of both the gravity and magnetic anomalies are using a rectangular prism approximation to simulate the presence of a strike-slip fault anomaly. These synthetic data modelling will provide guidance in identifying any offset that is captured by both the gravity and magnetic datasets, as shown in **Figure 3** (**Handyarso and Saleh, 2017; Handyarso, 2022, 2023**). The subsurface model is designed in such a way that there is a two-thirds offset within the causative body. This offset corresponds to a net-slip occurring approximately 70% of the width of the causative body. A comprehensive summary of the physical properties of the model, including its dimensions, density contrast, and susceptibility value is provided in **Table 1**. The model responses of both gravity and magnetic methods are calculated using a gravity equation for a rectangular prism proposed by Plouff and a magnetic equation for a rectangular prism proposed by Bhattacharyya respectively (**Blakely, 1995**). The resulting potential field represents the measured value at the surface. In the presence of offset within the causative bodies, this offset will be reflected as an anomaly pattern at the surface. Hence, the delineation of such patterns allows for the identification of strike-slip faults in the area.

The subsurface model consists of two blocky prisms that serve as sources of the anomaly bodies beneath the surface. Every single prism possesses identical physical properties such as density contrast or susceptibility. These two prisms are arranged in such a way to simulate the presence of a dextral strike-slip fault. The model is created using the real-world scale and is georeferenced under the UTM coordinates system. According to **Table 1**, the dextral strike-slip fault is located at Northing Y = 9197381.410 m with lateral movement in the west-east direction. The width of the causative bodies can be calculated using prism #1 as follows X1end – X1start = 254679.200 – 241572.080 = 13107.120 m. Similarly, if we calculate using prim #2, it becomes X2end – X2start = 263753.360 – 250646.240 = 13107.120 m. The net-slip is calculated using the start points of each prism as X2start – X1start = 250646.240 – 241572.080 = 9074.160 m. Similarly, if we calculate using the end points of each prism, it becomes X2end – X1end = 263753.360 – 254679.200 = 9074.160 m. In this case, the ratio of the net-slip to the width of the causative body is approximately 69.23%. In other words, the presence of net-slip amount in the synthetic modelling is approximately two-thirds of the width of the causative body. **Figure 3** showcases the visualization of the synthetic modelling, revealing a dextral strike-slip fault characterized by west-east lateral movement and north-south major axes, as specified in **Table 1**.

4. Results and Interpretations

The data analysis started with the examination of the Complete Bouguer Anomaly (CBA) and the Total Magnetic Intensity (TMI) anomaly, as shown in **Figure 4**. The CBA contains a wide range of values, spanning from -152.7 mGal to 291.2 mGal, reflecting its coverage of both land and marine areas. The CBA is characterized by a combination of low and high frequencies. The study area includes the Gulf of Tomini, which is surrounded by the Northern Arm and the Eastern Arm of Sulawesi. These arms form the northern and southern boundaries of the study area. The low CBA values are located around Gorontalo, Tomini, and Poso basins, while the high CBA values are found in the central part of the marine area. The high CBA values coincide with the existence of Togian and Una-Una islands, as well as the Lalanga Ridge, which is situated between Poso Basin and the Tomini Basin, as shown in **Figure 4** (left). The magnetic anomaly (TMI) is not associated with the basinal structures. The TMI anomaly ranges from -382.3 nT to 196.8 nT, with the high TMI anomaly concentrated in the center part of the study area. The strongest magnetic dipole pairs of the TMI anomaly are located at the Northern Arm of Sulawesi, as shown in **Figure 4** (right). The

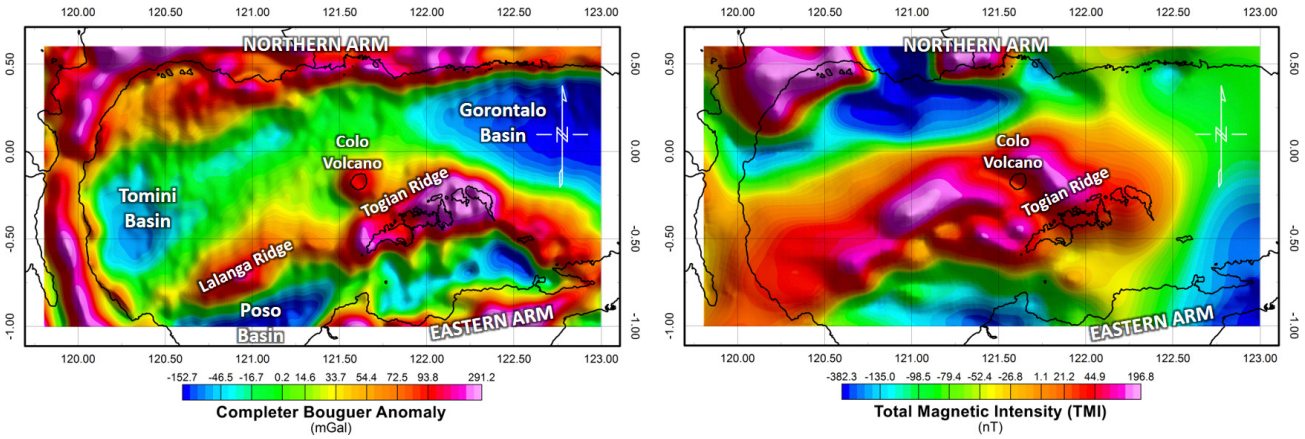

Figure 4: Gravity anomaly map (Complete Bouguer Anomaly-CBA) on the left, and magnetic anomaly map (Total Magnetic Intensity-TMI) on the right, superimposed with the coastline of the Gulf of Tomini, Northern Sulawesi, Indonesia

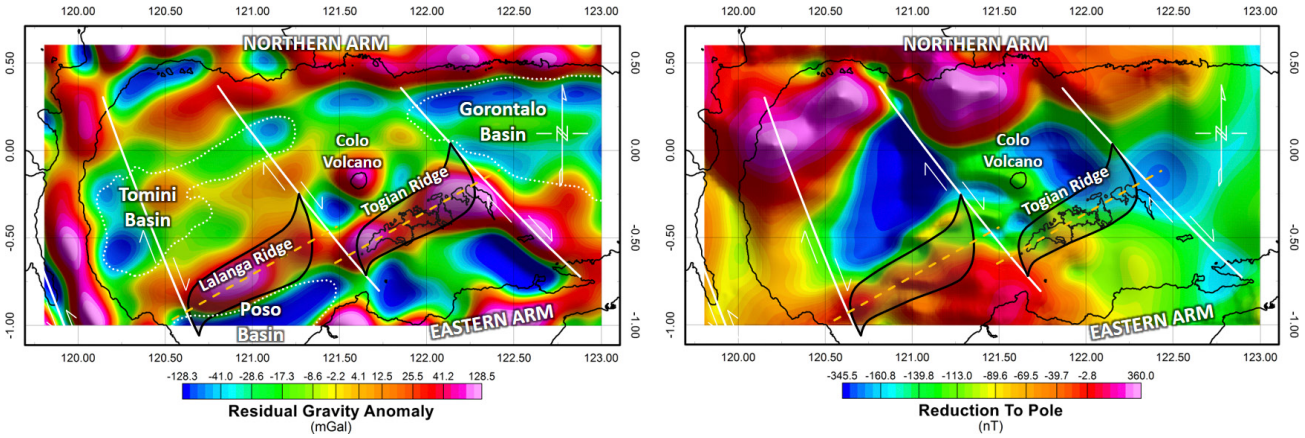

Figure 5: Residual gravity anomaly map (left) and the Reduction-to-Pole (RTP) map of the magnetic anomaly (right) are overlaid with the multiple parallel dextral strike-slip faults resulting from the analysis of gravity and magnetic datasets in this study

TMI anomaly characterizes a dipole pattern, while the CBA anomaly has a monopole pattern. As we can observe from the forward modelling case presented in **Figure 3**, despite our knowledge that the synthetic subsurface model represents a dextral strike-slip fault (see **Figure 3** top-left), there are no evident indications of this fault in the TMI anomaly (see **Figure 3** bottom-left). Hence, it is necessary to perform a prior correction on the TMI dipole anomaly to convert it into a monopole anomaly known as RTP before any interpretation can be made.

Structural interpretation can be conducted using both the residual gravity and the RTP magnetic anomaly dataset, as shown in **Figure 5**. The high residual gravity anomaly is predominantly located around the land area, while the low residual gravity anomaly is more prevalent in the marine water area. The highest RTP magnetic anomaly is concentrated in the northeastern part of the study area, while the low RTP magnetic anomaly is relatively located around the marine water area. Multiple parallel dextral strike-slip faults with a northwest-southeast trend direction are identified in the study area, widespread across the Gulf of Tomini. The general behavior of a strike-slip fault is characterized by the presence of offset or net-slip, which can be identified by analyzing the synthetic model responses obtained from both gravity and magnetic methods. The similar anomaly characteristic is also successfully identified from the field dataset of these two methods. There are several offsets identified in both the residual gravity anomaly and RTP magnetic anomaly, which are aligned in a northwest-southeast direction and spread across the study area, specifically the Gulf of Tomini, as shown in **Figure 5**. All of these offsets are interpreted as dextral strike-slip faults.

According to the residual gravity and the RTP anomaly maps, the identified multiple parallel dextral strike-slip faults from west to east (from left to right) consist of the Palu-Koro Fault zone, the Tambarana Fault zone, the Ampana Fault zone, the Buol Fault zone, and the Gorontalo Fault zone respectively. These fault zones show a relatively similar trend. The Palu-Koro Fault zone is characterized as a sinistral strike-slip fault, while the other fault zones are identified as dextral strike-slip faults. These multiple parallel dextral strike-slip faults with a northwest-southeast trend are driven by the extensional tectonics mechanism due to the clockwise rota-

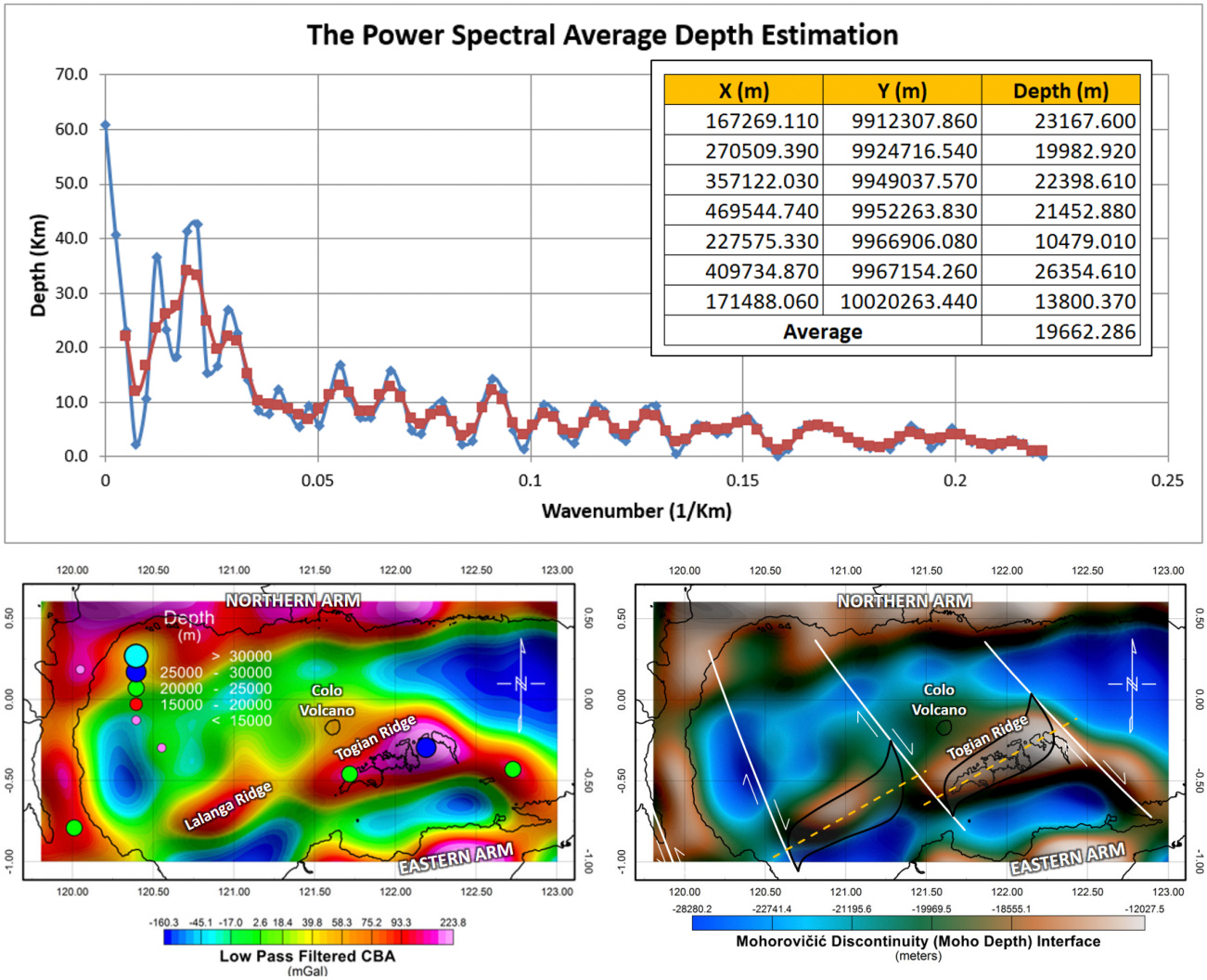

Figure 6: Power spectrum of the average depth curves plotted with a 3-points moving average (represented by a blue line) and 5-points moving average (represented by a red line) respectively. The power spectrum result is compared with the average depth of the 3D Euler deconvolution solutions under the UTM 51S zone projection in the table (top figure). The 3D Euler deconvolution depth solutions are overlaid with the low-pass filtered gravity anomaly (bottom left), while the Moho depth estimation result based on the Parker-Oldenburg algorithm is superimposed with the interpretation results (bottom right).

tion of the Northern Arm of Sulawesi. The eastern end of the Northern Arm acts as a pivot point in this rotation. The multiple parallel dextral strike-slip faults have triggered the rifting or opening in this area. The lateral movement of the rifting is relatively in the same direction as the multiple parallel dextral strike-slip faults, which is a northwest-southeast direction. However, the major axes of the opening area of the graben align in a northeast-southwest trend direction, which is relatively perpendicular to the direction of dextral strike-slip faults. The extensional tectonics mechanism has caused rifting or opening in the Gulf of Tomini, which is associated with the existence of the Togian and Lalanga ridges. These ridges coincide with high residual gravity anomaly but low RTP anomaly, as shown in **Figure 5**.

Further analysis was performed to enhance the current analysis of the gravity and magnetic datasets. An estimation of the average depth of the causative bodies was determined by utilizing the low-pass filtered CBA gravity data. The low-pass filtered CBA gravity data provide information about long wavelength anomalies, which represent the deeper portions of the causative bodies. Thus, the average depth obtained from the low-pass filtered datasets will provide an estimation of the deeper anomaly sources such as the Mohorovičić discontinuity depth. The average depth is derived using both spectral analysis and 3D Euler deconvolution, which represents the depth solutions of the point masses of the causative bodies. Two different filtering techniques were employed in the study. Regional-residual filtering was used to separate gravity data for the purpose of identifying structural lineaments, while low-pass filtering was utilized to detect deeper anomaly sources. The low-pass filtering is used to generate a long-wavelength gravity dataset, which is assumed to represent the Mohorovičić discontinuity (Moho) undulation interface.

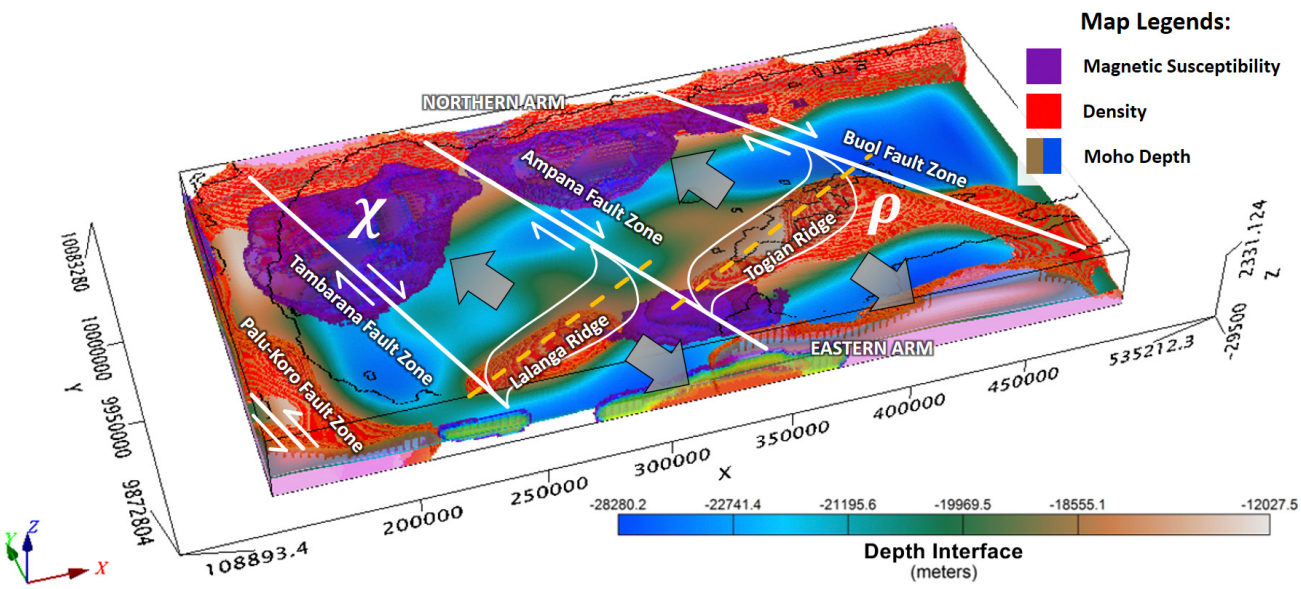

Figure 7: A 3D Perspective view of high-density contrast (ρ) bodies (coloured in red) and high susceptibility (χ) bodies (coloured in purple), superimposed on the undulation of the Mohorovičić discontinuity beneath the surface including structural interpretations in the area. The black lines represent the coastline in the study area, while the white lines represent interpretation of the geological structures as the result of the study.

A cut-off wavelength of 50.000 m (50 km) was utilized in the study. Another depth approximation is calculated through the use of 3D Euler deconvolution. The resulting solution locations are then listed in a table adjacent to the spectral analysis result and georeferenced under the UTM 51S zone projection (see **Figure 6** top). The average depth of the causative body obtained from the Radially Averaged Power Spectrum (RAPS) is approximately 20 km, while the average depth from the 3D Euler deconvolution is about 19662.286 m (19.662 km).

The solutions derived from 3D Euler deconvolution are divided into several classes marked with circles in different sizes and colors. All of these solutions are plotted over the low-pass filtered gravity anomaly results (see **Figure 6** bottom left). The estimation of Moho depth is calculated using an average depth value of about 20 km, and the density contrast between the crust and mantle is approximately 400 kg/m^3. The Moho depth and the corresponding interpretation results are shown in **Figure 6** (bottom right). It shows that the Moho topography exhibits variations around the average depth beneath the surface. The estimation of Mohorovičić discontinuity depth has revealed the presence of several areas with shallow Moho depth, including the Lalanga and Togian ridges. Another region with a deeper Moho depth is identified in the eastern part of the Togian Ridge and interpreted as the westward motion of the subduction zone of the Molucca Sea Plate (MSP), as shown in **Figure 6** (bottom right). In general, extensional tectonics cause the underlying mantle to uplift, decompress, and melt, resulting in shallow Moho depth. Additionally, the marine environment contributes to the rapid cooling of the rising magma and reduces its ability to penetrate further. The inferred rifting areas show major axes of the opening orientation in a northeast-southwest direction, coinciding with the presence of the Togian and Lalanga ridges. These two areas show high density anomalies but have a low magnetic susceptibility (see **Figure 5**), indicating that the rifting zones have been demagnetized due to the high temperatures associated with the uplift of the underlying mantle to the surface. The results show a good agreement with the fact that the Mohorovičić discontinuity becomes shallower around the rifting areas, as shown in **Figure 6**.

The subsurface modelling is obtained through a single 3D inversion process. This inversion is performed separately for the gravity and magnetic datasets. The gravity inverse modelling was conducted using low-pass filtered CBA gravity data, while the magnetic inverse modelling invoked the Reduction to Pole (RTP) magnetic data. The inversion results show an agreement with the current interpretations of the extensional tectonics in the study area, as shown in **Figure 7**. The red coloured zones highlight areas associated with a high-density body, while the purple-coloured zones indicate regions related to a high-susceptibility body. There are multiple parallel strike-slip faults spread across the study area. These faults can be identified by observing the lateral displacement or offset within the subsurface model, specifically in relation to both the density and susceptibility. The Mohorovičić discontinuity depth and the interpretation results are displayed together in a single frame or plot. The shallow Moho depth is superimposed on the high-density zones and Togian-Lalanga ridges, showing a northeast-southwest direction. Additionally, it is interpreted as the main axes of the rifting zones within the study area. Furthermore, this study incorporates the existing interpretations of geological structures on-land

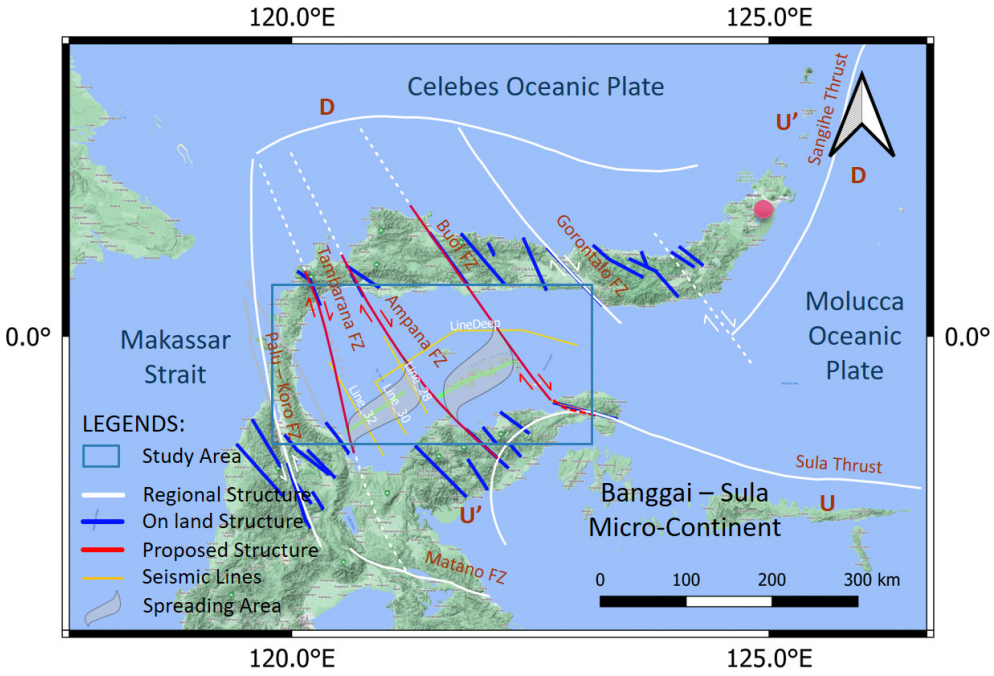

Figure 8: Redrawing of previous research on tectonic settings in the northern part of Sulawesi with consideration of extensional tectonics occurring in the Gulf of Tomini. The white lines represent the existing interpretation of the regional geological structures (**Walpersdorf et al., 1998b; Hinschberger et al., 2005; Pholbud et al., 2012**), the blue lines represent the existing interpretation of on-land geological structures (**Sidarto & Bachri, 2015**), and the red lines represent the multiple parallel dextral strike-slip faults identified in this study. The gray transparent area denotes the proposed rifting zone (opening area) based on gravity and magnetic datasets. The blue square represents the boundaries of the study area. The red circle at the eastern end of the Northern Arm of Sulawesi marks the pivot point of the clockwise rotation mechanism (**Song et al., 2022**).

with our results in the marine water area. By combining these findings, a comprehensive understanding of the tectonic settings is synthesized in the Gulf of Tomini.

The results obtained from the structural interpretation conducted in the Gulf of Tomini will enhance the existing interpretation of geological structure onshore. The information of structural environment in the Gulf of Tomini acquired from this study and was incorporated with the existing results of the previous studies (**Hamilton, 1979; Walpersdorf et al., 1998a; Djajadihardja et al., 2004; Rudyawan et al., 2014; White et al., 2014; Nugraha and Hall, 2018; Song et al., 2022**). The fault names identified in the marine area follow the existing fault names that have been defined on-land according to previous studies. The findings of this study are proposed to synthesize the overall tectonic settings in the northern part of Sulawesi, as shown in **Figure 8**. A previous study reported that in the early Miocene (around 23 Ma), the Sula spur began to collide with the Northern Arm of the Sulawesi volcanic arc and pushed north-westward. This collision eventually resulted in the welding of the Northern Arm and the Eastern part of Sulawesi into the West Sulawesi in the late Pliocene (2 Ma). As a result, the tectonic situation closely resembles the recent tectonic settings (see **Figure 1**). The Banggai-Sula moving northwestward collide, deformed, and lead to the following outcomes, such as the obduction of ophiolites in the Eastern Arm of Sulawesi and the clockwise rotation of the Northern Arm of Sulawesi with a pivot point at its eastern end (marked with a red circle in **Figure 8**). This clockwise rotation mechanism triggers the multiple parallel dextral strike-slip faults with a northwest-southeast direction and controls the extensional tectonics regime in the study area. The trend of these multiple parallel dextral strike-slip faults is relatively northwest-southeast direction, which is consistent with the kinematic plate movement vector with respect to the Sundaland (**Rangin et al., 1999; Baillie and Decker, 2022**).

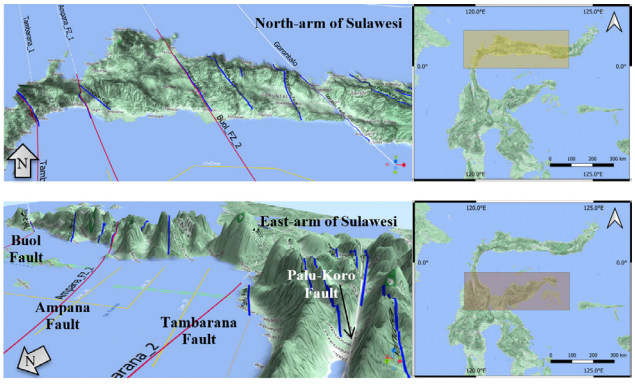

Figure 9: Perspective visualization in 3D of the Northern Arm (top) and the Eastern Arm (bottom) using DEM with a vertical exaggeration of about 15 in QGIS software. The visualization includes the overlaying of the existing interpretation of geological structures (represented by white and blue lines) and the proposed geological structures (represented by red lines). The gray arrows indicate the north direction.

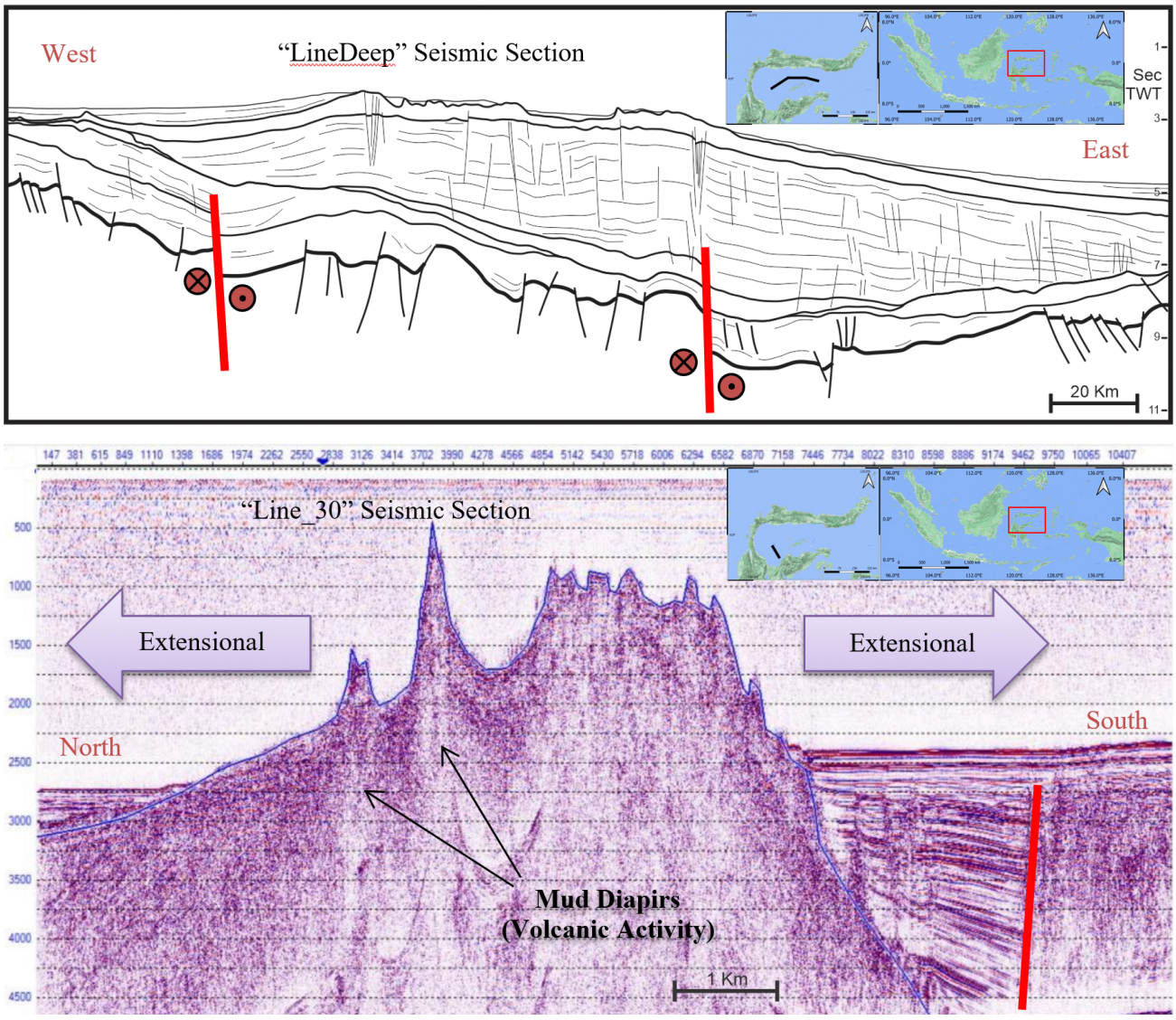

Figure 10: Two seismic sections show key features in the study area. "LineDeep" (top) is a 250 km long, 11 s two-way-traveltime (TWT) deep section and revealing normal faults perpendicular to the parallel dextral strike-slip faults. "Line_30" (bottom) spans 10 km, 4.5 s TWT, and showing volcanic mud-diapirs on the Lalanga ridge. Seismic line locations, namely "LineDeep" and "Line_30", are marked in the inset map and **Figure 8** (orange lines).

Extensional tectonics causes rifting or opening in several areas and results in the upwelling, decompressing, and melting of the underlying mantle. The seawater environment potentially influences the rapid cooling of the upwelling mantle. Thus, the rising mantle manifests as the shallow Moho depth interface and causes uplift in several locations. The uplift occurs in the Togian and Lalanga ridges, which are inferred as the main axes of the rifting zones with a northeast-southwest trend direction. Additionally, the seabed mapping reveals a bathymetric ridge for both Lalanga and Togian islands (**Pholbud et al., 2012**).

A DEM is visualized in 3D perspective to confirm any topographic evidence of faulting system identified in the study area. Fault can be revealed by using topographic relief analysis (**Florinsky, 1996**). According to **Figure 8**, this study proposed the presence of multiple dextral strike-slip faults extending across the Gulf of Tomini. These faults are identified as connecting or linking the Northern Arm and the Eastern Arm of Sulawesi. The multiple parallel dextral strike-slip faults deduced from the analysis of gravity and magnetic datasets in the Gulf of Tomini are interpreted as extension faults (represented by red lines). These faults are thought to have originated from the existing interpretation of geological structures on-land (represented by blue lines) and the known regional structures (represented by white lines). A superimposed visualization of the DEM with the geological structures demonstrates notable consistency with the topographic relief observed in the area, as shown in **Figure 9**. The superimposed visualization includes the existing fault structures (the white and blue lines) and the interpretation results of this study (the red lines).

5. Discussion

The research has yielded several significant findings that need to be emphasized. One of these findings is the identification of extensional tectonics through the analysis of gravity and magnetic datasets. Furthermore, the interpretation is validated or confirmed by the existing seismic sections. The seismic sections referred to as "LineDeep" (**Rudyawan et al., 2014**) and "Line_30" (**Kusnida, 2008; Kusnida & et al., 2012; Subarsyah & Sahudin, 2016**) are shown in **Figure 10** respectively. The positions and orientations of the line locations are displayed on the map in **Figure 8**. These two figures serve different purposes but are generally used as constraints in the interpretation of the results of our current work. The first seismic section, "LineDeep" is a long and deep section with a west-east direction, revealing several normal faults that correspond to multiple parallel dextral strike-slip faults in the northwest-southeast trend direction. The red lines in **Figure 10** (top) indicate these dextral strike-slip faults. The dot sign denotes the side moving forward to (or approaching) the reader of the paper, while the cross sign indicates movement backward to leave away from the reader. This seismic line is interpreted into various rock units, but they are not discussed in this paper. Detailed information is suggested to be referred to the original work directly (**Rudyawan et al., 2014**). Another seismic section, "Line_30" is located at the Tomini Bay, crossing the Lalanga Ridge and has a northwest-southeast line direction. This seismic section exposes the extensional tectonic settings, which generate a graben structure with indications of the mud-volcanoes / mud-diapirs located in the middle of the rifting zones around the study area. The mud-volcanoes or mud-diapirs are identified as the chaotic seismic section, characterized by a taper structural pattern observed in the seismic section, as shown in **Figure 10** (bottom). Previously, it was interpreted as pinnacle reefs (**Pholbud et al., 2012**).

The multiple parallel dextral strike-slip faults identified in the study area are caused by the clockwise rotation of the Northern Arm of Sulawesi, where its eastern end behaves as the pivot-point and the rotation is confined by the Palu-Koro and Lawanopo fault systems. These types of tectonic movements trigger extensional tectonics and cause rifting or opening in the area. As a result, the underlying mantle rises and manifests as the Togian and Lalanga ridges. The existence of a normal fault observed in the seismic section "Line_30", which is located crossing the Lalanga Ridge, as shown in **Figure 10** (bottom), serves as evidence supporting the occurrence of extensional tectonics. The graben structure is found in the southern portion of the line, while the Lalanga Ridge is situated in the northern portion. The weak zone of the rifting area is located relatively in the northern side of the mentioned normal fault. This weak zone has experienced intrusion by the activity of mud-volcanoes (mud-diapirs), resulting in the development of the Lalanga Ridge. By using these two seismic sections, it was demonstrated that the interpretation results of the current work presented in the paper are well matched with the existing seismic section as our constraints.

The study area is inferred as a transitional marine rift based on the inference that the Moho depth interface is approximately 20 km, which is thicker than oceanic crust but thinner than typical continental crust. Typically, the Moho depth in the oceanic crust is less than or equal to 10 km, whereas in the continental crust area, it commonly ranges between 20-70 km. The Moho depth of about 20-30 km is often associated with the transitional zone. In a transitional marine rift, there are several factors that can trigger the occurrence of mud-diapirs or mud-volcanoes. The process of crustal extension or crustal thinning in a rift zone results in the stretching and thinning of the Earth's crust. This leads to the development of grabens or half-grabens and may trigger the upwelling of the underlying asthenosphere. The graben or half-graben behaves as a depositional area, facilitating the accumulation of fine-grained mud. During a long period of sedimentation, a thick and water-saturated sedimentary sequence can be formed, providing a potential source for mud mobilization and upward migration. The composition and properties of the subsurface geology, including the presence of clay-rich or fine-grained sediments can influence the formation of mud-volcanoes and mud-diapirs. Certain lithological and stratigraphic conditions can promote the accumulation and mobilization of mud. The extensional tectonics can yield faults that serve as pathways for the ascent of fluids, including mud from deeper sedimentary layers. Fault zones may act as conduits for the ascent of mud, allowing mud to migrate towards the surface and leading to the formation as mud-volcanoes or mud-diapirs. The upwelling of the underlying mantle results in a higher gravity anomaly compared to its surroundings. In some rift areas, hydrothermal activity may be present due to the interaction between hot fluids and the subsurface geology. Hydrothermal fluids can mobilize and transport mud, contributing to the formation of mud-volcanoes or mud-diapirs. The existence of submarine hydrothermal activity is also confirmed by a previous study on geochemistry, which successfully identified a manganese-rich sediment layer in the Gulf of Tomini (**Yuliyanti et al., 2022**).

The extensional tectonic is still ongoing up to the present time, where the Palu-Koro and Lawanopo fault zone serve as the boundary for the rotational tectonic movements (**Socquet et al., 2006; Baillie and Decker, 2022**). The monitoring of the Palu-Koro Fault using GPS and earthquake slip vector data shows that the southern (or western) area of the Palu-Koro Fault shows small relative motion (< 2 mm/year) with respect to Sundaland. However, in the northern (or eastern) area of the fault system, the relative motion varies from 11 to 42

mm/year (**Socquet et al., 2006; Baillie and Decker, 2022**). The Banggai-Sula Microcontinent moves northwestward and collides with Sulawesi Island, resulting in the obduction of ophiolites over the Eastern Arm of Sulawesi. However, these processes initiated with a short period of subduction, leading to the belief that remnants of the Banggai-Sula Microcontinent still exist beneath the Eastern Arm of Sulawesi (**Walpersdorf et al., 1998a; Darman, 2011; Pholbud et al., 2012**). Hypothetically, the North Banda Sea Basin also moves in a north-westward direction and exerts pressure on the Palu-Koro-Lawanopo faulting system. Hence, the extensional tectonic settings in the Gulf of Tomini are primarily controlled by the Palu-Koro-Lawanopo faulting system, which is influenced by the north-westward movement of the North Banda Sea Basin Plate. In contrast, the Banggai-Sula Microcontinent is postulated to show a slight contrasting behaviour, potentially causing shortening tectonics instead of extensional tectonics in the area. The Banggai-Sula Microcontinent has the potential to exert pressure on the Matano Fault zone, indirectly influencing the Palu-Koro faulting system, thereby contributing to the extensional tectonics observed in the Gulf of Tomini. The occurrence of shortening tectonics can suppress volcanic activity in the area, whereas extensional tectonics can trigger new volcanic activity. Both processes are presence in the Gulf of Tomini. The presence of multiple parallel dextral strike-slip faults serves as evidence of the segmentation of the Northern Arm of Sulawesi, resulting from its clockwise rotation. A further study is needed to compare the kinematic movement based on time-lapse GPS measurements of both the Palu-Koro-Lawanopo faulting system and the Banggai-Sula Microcontinent with reference to the southern (or western) area of the Palu-Koro Fault, which represents the Eurasian Continental Plate (ECP).

6. Conclusions

The study area, encompassing the Gulf of Tomini is inferred as a transitional marine rift. This inference is supported by the observed variation in the Moho depth interface, which ranges approximately 12-28 km beneath the surface. Additionally, the presence of extensional tectonics has been successfully identified through the occurrence of multiple parallel dextral strike-slip faults that show a northwest-southeast trend direction spread across the area. These fault lineaments are recognized based on the synthetic data modelling of both gravity and magnetic anomaly responses. The interpretation results obtained from the analysis of gravity and magnetic show a good agreement with the existing seismic sections used as constraints in the study area. The multiple parallel dextral strike-slip faults are controlled by the clockwise rotational tectonics of the Northern Arm of Sulawesi, with its Eastern end acting as the pivot point. These tectonic movements trigger the extensional tectonic mechanism, resulting in crustal thinning around the study area. This process leads to several outcomes, including the development of graben and fault structures known as the Gorontalo, Tomini, and Poso basins. Additionally, it influences the presence of mud-volcanoes or mud-diapirs (and possibly volcanic activity) around the Lalanga and Togian ridges, including Una-Una Island (Colo Volcano). The rising, decompressing, and melting of the underlying mantle is reflected in shallow Moho depths, which also coincide with the Lalanga and Togian ridges. The graben structures serve as depositional areas and facilitate the accumulation of fine-grained mud as water-saturated sedimentary sequences. Meanwhile, faults act as pathways for the upward migration of the ascent of fluids (mud) to the surface, forming mud-diapirs or mud-volcanoes. The Lalanga and Togian ridges are inferred to represent the opening area with the major axes showing a northeast-southwest direction that is relatively perpendicular to the trend of the multiple dextral strike-slip faults. This research has the capability to accurately determine the regional tectonic settings and makes a significant contribution in guiding exploration activities effectively. One particular benefit of the research is the identification and exposure of existing mud-diapirs within the study area, which is considered highly advantageous. This knowledge has the potential to reduce exploration risks, especially in oil and gas exploration because distinguishing between reef-building and mud-diapirs can be challenging. Additionally, a comprehensive understanding of the volcanic environment would significantly enhance mineral ore exploration in the future, particularly considering that the majority of the Indonesian region is comprised of volcanic areas.

Acknowledgement

The authors express their utmost gratitude to the anonymous reviewers for their constructive suggestions in enhancing the quality of this paper and special appreciation is extended to the open-minded editors of the journal.

7. References

Papers:

Ardestani, V. E. and Mousavi, N. (2023): The Moho Relief Beneath the Zagros Collision Zone Through Modeling of Ground-Based Gravity Data and Utilizing Open-Source Resources in Python. Pure and Applied Geophysics, 180, 909–918. https://doi.org/10.1007/s00024-022-03221-7

Ashena, Z. B., Ardestani, V. E., Camacho, A. G., Dehghani, A., and Fernández, J. (2018): Moho Depth Determination beneath the Zagros Mountains from 3D Inversion of Gravity Data. Arabian Journal of Geosciences, 11(52), 1–12. https://doi.org/10.1007/s12517-018-3385-x

Baillie, P. and Decker, J. (2022): Enigmatic Sulawesi: The Tectonic Collage. Berita Sedimentologi, 48(1), 1–30. https://doi.org/10.51835/bsed.2022.48.1.388

Beiki, M. (2010): Analytic Signals of Gravity Gradient Tensor and Their Application to Estimate Source Location. Geophysics, 75(6), 159–174. https://doi.org/10.1190/1.3493639

Chen, W., Tenzer, R., Xu, X., Wang, S., and Wang, B. (2021): Moho Depth Estimation Beneath Tibet from Satellite Gravity Data Based on a Condensation Approach. Earth and Space Science, 8(6), 1–19. https://doi.org/10.1029/2020EA001261

Cottam, M. A., Hall, R., Forster, M. A., and Boudagher-Fadel, M. K. (2011): Basement Character and Basin Formation in Gorontalo Bay, Sulawesi, Indonesia: New Observations from the Togian Islands. Geological Society Special Publication, 355(July 2015), 177–202. https://doi.org/10.1144/SP355.9

Darman, H. (2011): Seismic Expression of North Sulawesi Subduction Zone. Berita Sedimentologi, 22(10), 5–8. https://journal.iagi.or.id/index.php/FOSI/article/view/198/168

Djajadihardja, Y. S., Taira, A., Tokuyama, H., Aoike, K., Reichert, C., Block, M., Schluter, H. U., and Neben, S. (2004): Evolution of an Accretionary Complex along the North Arm of the Island of Sulawesi, Indonesia. The Island Arc, 13(1), 1–17. https://doi.org/10.1111/j.1440-1738.2003.00403.x

Florinsky, I. V. (1996): Quantitative Topographic Method of Fault Morphology Recognition. Geomorphology, 16(2), 103–119. https://doi.org/10.1016/0169-555X(95)00136-S

Fullea, J., Fernàndez, M., and Zeyen, H. (2008): FA2BOUG–A FORTRAN 90 Code to Compute Bouguer Gravity Anomalies from Gridded Free-Air Anomalies: Application to the Atlantic-Mediterranean Transition Zone. Computers and Geosciences, 34(12), 1665–1681. https://doi.org/10.1016/j.cageo.2008.02.018

Ghalehnoee, M. H., Ansari, A., and Ghorbani, A. (2017): Improving Compact Gravity Inversion Using New Weighting Functions. Geophysical Journal International, 208(1), 546–560. https://doi.org/10.1093/gji/ggw413

Golshadi, Z., Ramezanali, A. K., and Kafaei, K. (2016): Interpretation of Magnetic Data in the Chenar-e Olya Area of Asadabad, Hamedan, Iran, Using Analytic Signal, Euler Deconvolution, Horizontal Gradient, and Tilt Derivative Methods. Bollettino di Geofisica Teorica ed Applicata, 57(4), 329–342. https://doi.org/10.4430/bgta0182

Gómez-Ortiz, D. and Agarwal, B. N. P. (2005): 3DINVER.M: A MATLAB Program to Invert the Gravity Anomaly over a 3D Horizontal Density Interface by Parker-Oldenburg's Algorithm. Computers and Geosciences, 31(4), 513–520. https://doi.org/10.1016/j.cageo.2004.11.004

Hall, R. (2012): Late Jurassic-Cenozoic Reconstructions of the Indonesian Region and the Indian Ocean. Tectonophysics, 570–571, 1–41. https://doi.org/10.1016/j.tecto.2012.04.021

Hamilton, W. (1979): Tectonics of the Indonesian Region. Bulletin of the Geological Society of Malaysia, 6(July), 3–10. https://doi.org/10.7186/bgsm06197301

Handyarso, A. (2022): Ring-Fault Delineation of an Ancient Volcanic Caldera Based on 3-D Gravity Inverse Modeling in Majenang Region, Indonesia. Kurvatek, 7(2), 103–114. https://doi.org/10.33579/krvtk.v7i2.3197

Handyarso, A. (2023): Caldera-Like Delineation and Geological Resources Identification of Majenang Area, Indonesia by Gravity and Magnetic Data Inversions. *(Submitted)*.

Handyarso, A. and Saleh, H. M. (2017): Strike-Slip Fault Identification Beneath of the Wiriagar Oil Field. Scientific Contribution Oil and Gas, 40(3), 133–144. https://doi.org/10.29017/SCOG.40.3.51

Hinschberger, F., Malod, J. A., Réhault, J. P., Villeneuve, M., Royer, J. Y., and Burhanuddin, S. (2005): Late Cenozoic Geodynamic Evolution of Eastern Indonesia. Tectonophysics, 404(1–2), 91–118. https://doi.org/10.1016/j.tecto.2005.05.005

Katili, J. A. (1978): Past and Present Geotectonic Position of Sulawesi, Indonesia. Tectonophysics, 45(4), 289–322. https://doi.org/10.1016/0040-1951(78)90166-X

Katili, J. A., Kartaadiputra, L., and Surio. (1963): Magma Type and Tectonic Position of the Una-Una Island, Indonesia. Bulletin Volcanologique, 26(1), 431–454. https://doi.org/10.1007/BF02597303

Kopp, C., Flueh, E. R., and Neben, S. (1999): Rupture and Accretion of the Celebes Sea crust Related to the North-Sulawesi Subduction: Combined Interpretation of Reflection and Refraction Seismic Measurements. Journal of Geodynamics, 27(3), 309–325. https://doi.org/10.1016/S0264-3707(98)00004-0

Kunnummal, P., Anand, S. P., Haritha, C., and Rama Rao, P. (2018): Moho Depth Variations over the Maldive Ridge and Adjoining Arabian and Central Indian Basins, Western Indian Ocean, from Three Dimensional Inversion of Gravity Anomalies. Journal of Asian Earth Sciences, 156, 316–330. https://doi.org/10.1016/j.jseaes.2017.12.012

Kusnida, D. and Subarsyah (2008): Deep Sea Sediment Gravity Flow Deposits in Gulf of Tomini, Sulawesi. Indonesian Journal on Geoscience, 3(4), 217–224. https://doi.org/10.17014/ijog.vol3no4.20084

Kusnida, D., Subarsyah, and Nirwana, B. (2009): Basement Configuration of the Tomini Basin Deduced from Marine Magnetic Interpretation. Indonesian Journal on Geoscience, 4(4), 269–274. https://doi.org/10.17014/ijog.vol4no4.20094

Lefort, J. P. and Agarwal, B. N. P. (2000): Gravity and Geomorphological Evidence for a Large Crustal Bulge Cutting Across Brittany (France): A Tectonic Response to the Closure of the Bay of Biscay. Tectonophysics, 323(3–4), 149–162. https://doi.org/10.1016/S0040-1951(00)00103-7

Nugraha, A. M. S. and Hall, R. (2018): Late Cenozoic Palaeogeography of Sulawesi, Indonesia. Palaeogeography, Palaeoclimatology, Palaeoecology, 490(November 2017), 191–209. https://doi.org/10.1016/j.palaeo.2017.10.033

Parang, S., Safari, A., Sharifi, M. A., and Bahrodi, A. (2016): Moho Depth Estimation Using Gravitational Gradient Tensor (GGT) and 3D Euler Deconvolution Algorithm. Living Planet Symposium (LPS) 2016, 1–3. https://lps.esa.int/page_paper0779

Parlak, A. Y. and Elmas, A. (2023): Architecture of Tectonic and Crustal Structure of the Middle Marmara Sub-Basin and Its Surroundings Using Gravity Data. Carbonates and Evaporites, 38(3), 1–12. https://doi.org/10.1007/s13146-022-00830-0

Pholbud, P., Hall, R., Advokaat, E., Burgess, P., and Rudyawan, A. (2012): A New Interpretation of Gorontalo Bay, Sulawesi. Proceedings, Indonesian Petroleum Association, 36(May).

Pigram, C. J. and Panggabean, H. (1984): Rifting of the Northern Margin of the Australian Continent and the Origin of Some Microcontinents in Eastern Indonesia. Tectonophysics, 107(3–4), 331–353. https://doi.org/10.1016/0040-1951(84)90257-9

Puntodewo, S. S. O., McCaffrey, R., Calais, E., Bock, Y., Rais, J., Subarya, C., Poewariardi, R., Stevens, C., Genrich, J., Fauzi, Zwick, P., Wdowinski, S. (1994): GPS Measurements of Crustal Deformation within the Pacific-Australia Plate Boundary Zone in Irian Jaya, Indonesia. Tectonophysics, 237(3–4), 141–153. https://doi.org/10.1016/0040-1951(94)90251-8

Rachman, G., Santosa, B. J., Nugraha, A. D., Rohadi, S., Rosalia, S., Zulfakriza, Z., Sungkono, S., Sahara, D. P., Muttaqy, F., Supendi, P., Ramdhan, M., Ardianto, A., and Afif, H. (2022): Seismic Structure Beneath the Molucca Sea Collision Zone from Travel Time Tomography Based on Local and Regional BMKG Networks. Applied Sciences (Switzerland), 12(20). https://doi.org/10.3390/app122010520

Rangin, C., Pichon, X. L., Mazzotti, S., Pubellier, M., Chamot-Rooke, N., Aurelio, M., Walpersdorf, A., and Quebral, R. (1999): Plate Convergence Measured by GPS across the Sundaland/Philippine Sea Plate Deformed Boundary: The Philippines and Eastern Indonesia. Geophysical Journal International, 139(2), 296–316. https://doi.org/10.1046/j.1365-246X.1999.00969.x

Rao, V. B. and Satyanarayana Murty, B. V. (1973): Note on Parasnis' Method for Surface Rock Densities. Pure and Applied Geophysics PAGEOPH, 110(1973/IX), 1927–1931. https://doi.org/10.1007/BF00876555

Reid, A. B. (1998): Prospect Scale Interpretation of HRAM Data : Euler Depth Estimates. Canadian Journal of Exploration Geophysics, 34(1–2), 23–29. https://csegjournal.com/archives/1998-12

Reid, A. B., Allsop, J. M., Granser, H., Millett, A. J., and Somerton, I. W. (1990): Magnetic Interpretation in Three Dimensions using Euler Deconvolution. Geophysics, 55(1), 80–91. https://doi.org/10.1190/1.1442774

Rudyawan, A., Hall, R., and White, L. (2014): Neogene Extension of the Central North Arm of Sulawesi, Indonesia. *AGU Fall Meeting December 2014*, (September), 2–3. https://doi.org/10.13140/RG.2.1.2893.8962

Sendjaja, P., Suparka, E., Abdullah, C. I., and Sucipta, I. G. B. E. (2020): Characteristic of the Mount Colo Volcano, Una-Una Island, Central Sulawesi Province: Tectonic Evolution and Disaster Mitigation. IOP Conference Series: Earth and Environmental Science, 589(1), 1–8. https://doi.org/10.1088/1755-1315/589/1/012005

Silver, E. A., McCaffrey, R., and Smith, R. B. (1983): Collision, Rotation, and the Initiation of Subduction in the Evolution of Sulawesi, Indonesia. Journal of Geophysical Research, 88(B11), 9407–9418. https://doi.org/10.1029/JB088iB11p09407

Socquet, A., Simons, W., Vigny, C., McCaffrey, R., Subarya, C., Sarsito, D., Ambrosius, B., and Spakman, W. (2006): Microblock Rotations and Fault Coupling in SE Asia Triple Junction (Sulawesi, Indonesia) from GPS and Earthquake Slip Vector Data. Journal of Geophysical Research: Solid Earth, 111(B8), 1–15. https://doi.org/10.1029/2005JB003963

Song, T., Hao, T., Zhang, J., Cao, L., and Dong, M. (2022): Numerical Modeling of North Sulawesi Subduction Zone: Implications for the East–West Differential Evolution. Tectonophysics, 822(November 2021), 229172. https://doi.org/10.1016/j.tecto.2021.229172

Subarsyah, S. and Sahudin, S. (2016): Identifikasi Sub-Cekungan di Cekungan Tomini Bagian Selatan, Berdasarkan Penampang Seismik 2D dan Anomali Gaya Berat. Jurnal Geologi Kelautan, 8(2), 95. https://doi.org/10.32693/jgk.8.2.2010.190

Martosuwito, Surono (2012): Tectonostratigraphy of the Eastern Part of Sulawesi, Indonesia. In Relation to the Terrane Origins. Jurnal Geologi dan Sumberdaya Mineral (JGSM), 22(4), 199–207.

Thompson, D. T. (1982): EULDPH: A New Technique for Making Computer-Assisted Depth Estimates from Magnetic Data. Geophysics, 47(1), 31. https://doi.org/10.1190/1.1441278

Walpersdorf, A., Rangin, C., and Vigny, C. (1998a): GPS Compared to Long-term Geologic Motion of the North Arm of Sulawesi. Earth and Planetary Science Letters, 159(1–2), 47–55. https://doi.org/10.1016/S0012-821X(98)00056-9

Walpersdorf, A, Vigny, C., Subarya, C., and Manurung, P. (1998b). Monitoring of the Palu-Koro Fault (Sulawesi) by GPS. Geophysical Research Letters, *25*(13), 2313–2316. https://doi.org/10.1029/98GL01799

Watkinson, I. M., Hall, R., Cottam, M. A., Sevastjanova, I., Suggate, S., Gunawan, I., Pownall, J. M., Hennig, J., Ferdian, F., Gold, D., Zimmermann, S., Rudyawan, A., and Advocaat, E. (2012): New Insights into the Geological Evolution of Eastern Indonesia from Recent Research Projects by the SE Asia Research Group. Berita Sedimentologi, 23(January 2012), 21–27. https://journal.iagi.or.id/index.php/FOSI/article/view/189/159

White, L. T., Hall, R., and Armstrong, R. A. (2014): The Age of Undeformed Dacite Intrusions within the Kolaka Fault Zone, SE Sulawesi, Indonesia. Journal of Asian Earth Sciences, 94, 105–112. https://doi.org/10.1016/j.jseaes.2014.08.014

Yudistira, T. and Grandis, H. (1998): Interpretasi Gravitasi dan Magnetik Menggunakan Metode Sinyal Analitik dan Dekonvolusi Euler 3-D. *Proceeding HAGI*, (1971), 7–8.

Yuliyanti, A., Permana, H., Setiawan, I., Nurohman, H., and Saputro, S. P. (2022): Geochemistry of Seafloor Surface Sediment and Submarine Hydrothermal Signature of Tomini Bay, Indonesia. Australian Journal of Earth Sciences, 69(7), 1000–1011. https://doi.org/10.1080/08120099.2022.2082529

Chapters in books or proceedings with editor(s):

Oldenburg, D. W. and Li, Y. (2005): 5. Inversion for Applied Geophysics: A Tutorial. In: Butler, D. K. (eds.): Near-

Surface Geophysics. – Society of Exploration Geophysicists., 89–150, 733 p. https://doi.org/10.1190/1.9781560801719.ch5

Sidarto and Bachri, S. (2015): Bagian VI, Struktur Geologi dan Tektonik; Bab XII, Struktur Geologi. In: Martosuwito, S. and Hartono, U. (eds.): Geologi Sulawesi (Second Edition). – LIPI Press., 277–302, 352 p.

Books/thesis:

Blakely, R. J. (1995): Potential Theory in Gravity and Magnetic Applications. In Cambridge University Press, 441 p. https://doi.org/10.1017/CBO9780511549816

Grandis, H. (2009): Pengantar Pemodelan Inversi Geofisika. Himpunan Ahli Geofisika Indonesia (HAGI), Bandung, 186 p.

Kusnida, D., Silalahi, I. R., Naibaho, T., and Subarsyah. (2012): Marine Geological Investigations in the Tomini Basin, Central Sulawesi. Marine Geological Institute, Research and Development Agencies for Energy and Mineral Resources, Ministry of Energy and Mineral Resources (MEMR) of the Republic of Indonesia, Jakarta, 35 p.

Internet sources:

CCOP., CCGPESA., and GSJ. (2021): Magnetic Anomaly Map of East and Southeast Asia Revised Version 3 (3rd Edition). http://www.ccop.or.th/publication-details/97

Oceanography, S. I. O. (2023): EXTRACT XYZ GRID - TOPOGRAPHY OR GRAVITY. Retrieved from University of San Diego website: https://topex.ucsd.edu/cgi-bin/get_data.cgi (accessed 22nd December 2021)

SAŽETAK

Istraživanje ekstenzijske tektonike temeljeno na analizi gravimetrijskih i magnetskih podataka u zaljevu Tomini, Indonezija

Zagonetka otoka Sulawesi i dalje je tema rasprave među znanstvenicima. Sjeverni krak Sulawesija označen je kao vulkanska provincija, dok je istočni krak identificiran kao ofiolitna zona zajedno s nekoliko mikrokontinentalnih fragmenata. Međutim, tektonski odnos u morskome području između tih dvaju krakova nije jasno definiran. Postojanje izoliranih vulkanskih otoka, odnosno otoka Una-Una i Togian, pridonosi kompleksnosti područja i nalaže potrebu za regionalnim istraživanjima koja se koriste gravimetrijskim i magnetskim metodama u zaljevu Tomini, Sjeverni Sulawesi, Indonezija. Stoga je provedena sveobuhvatna analiza koja je uključivala 3D inverzno modeliranje i procjenu dubine Moho diskontinuiteta na temelju Parker-Oldenburgova algoritma korištenjem 3D Eulerove dekonvolucije kako bi se dobila prosječna dubina uzročnika anomalije. Kao rezultat toga, prisutnost ekstenzijske tektonike otkrivena je i identificirana u obliku višestrukih paralelnih dekstralnih rasjeda na području istraživanja. Svi rasjedi koji pokazuju lineamente sjeverozapad-jugoistok u skladu su s postojećim seizmičkim profilima. Mehanizmi ekstenzijske tektonike pokrenuli su stanjenje kore i rascjepe, što je dovelo do nastanka grabenskih struktura kao što su bazeni Gorontalo, Tomini i Poso. Nadalje, utjecali su i na vulkansku aktivnost oko otoka Togian i Una-Una. Glavne osi pretpostavljenoga otvora orijentirane su u smjeru sjeveroistok-jugozapad, okomito na lineamente rasjeda. Područje otvaranja podudara se s orijentacijom grebena Lalanga i Togian. Na kraju, prikazana je regionalna geološka struktura preko zaljeva Tomini koja povezuje sjeverni i istočni rukavac Sulawesija.

Ključne riječi:
gravimetrija, magnetometrija, Mohorovičićev diskontinuitet, ekstenzijska tektonika, bazen Gorontalo-Tomini

Authors' contribution

Accep Handyarso (1) carried out gravity and magnetic data collection, performed the data processing up to the interpretation results, literature review, and was in charge of manuscript writing. **Haryadi Permana (2)** provided the existing geological structure interpretations around the study area for consideration, such as several fault maps and the existing fault names for the whole study area. **Mustafa Hanafi (3)** provided seismic dataset, processing, and its interpretations, which express the possibility of volcanic characteristics found in the study area based on marine seismic survey. **Purnama Sendjaja (4)** provided literature study, especially about the origin of Una-Una or the Colo Volcano in the study area. **Muhammad Maruf Mukti (5)** provided several pictures of the Digital Elevation Model (DEM) to confirm the fault zones in the interpretation of the results with the on-land geological structures.